PHYSICAL REVIEW A **87**, 022326 (2013)

Near-deterministic quantum teleportation and resource-efficient quantum computation using linear optics and hybrid qubits

Seung-Woo Lee[1] and Hyunseok Jeong[1,2,*]

[1]*Center for Macroscopic Quantum Control, Department of Physics and Astronomy, Seoul National University, Seoul 151-742, Korea*

[2]*Centre for Quantum Computation and Communication Technology, School of Mathematics and Physics, University of Queensland, Brisbane, Queensland 4072, Australia*

(Received 20 March 2012; revised manuscript received 20 December 2012; published 19 February 2013)

We propose a scheme to realize deterministic quantum teleportation using linear optics and hybrid qubits. It enables one to efficiently perform teleportation and universal linear-optical gate operations in a simple and near-deterministic manner using all-optical hybrid entanglement as off-line resources. Our analysis shows that our approach outperforms previous ones when considering both the resource requirements and fault-tolerance limits.

DOI: 10.1103/PhysRevA.87.022326 PACS number(s): 03.67.Lx, 42.50.−p

I. INTRODUCTION

Quantum computers are expected to offer phenomenal increases of computational power over classical computers [1]. There are many different approaches to implementations of quantum computers based on various physical systems while scalable quantum computation in a fault-tolerant manner is still beyond current technology. Optical models have some prominent advantages such as relatively quick operational time compared to decoherence time [2–4]. However, massive resource requirements and the gap between the fault-tolerance limit and the realistic error rate should be significantly reduced [4].

Certain properties of light can be useful to implement qubits for optical quantum information processing. Typically, photons as "particles of light" are considered to encode information with a well-chosen degree of freedom such as horizontal and vertical polarization states, $|H\rangle$ and $|V\rangle$. A major difficulty in this approach is to realize two-qubit gates since photons seldom interact with each other, while single-qubit operations are straightforward [2–4]. In principle, scalable quantum computation can be achieved without inline nonlinear interactions [5], which is often called linear optical quantum computing (LOQC).

However, its practical implementation is difficult because LOQC gates are inherently nondeterministic [5]. In the context of LOQC, quantum teleportation can be used to perform demanding two-qubit gates using the gate teleportation protocol. However, the Bell-state measurement, which forms the key element of the teleportation protocol, cannot be performed deterministically using linear optics in this approach. Only two of the four Bell states can be identified and thus the success probability cannot exceed 50% [6]. It requires a very large number of resources in order to increase the success probability of gate operations for quantum computing [5] or that of the Bell-state measurement itself [7].

In general, any two distinct field states can be explored for a qubit basis [4]. Along this line, the coherent-state quantum computing (CSQC) has been developed with its own merit [8–12]. In CSQC, two coherent states, $|\alpha\rangle$ and $|-\alpha\rangle$ with amplitudes $\pm\alpha$, are used to form a qubit basis, and equal superpositions of coherent states, e.g., $|\alpha\rangle + |-\alpha\rangle$ [13], are required as resources [11]. Using this encoding scheme, the Bell-state measurement for coherent-state qubits (B_α) can be performed in a near-deterministic manner as α gets large [8]. However, a necessary single-qubit operation, i.e., Z rotations, produces a cumbersome type of error due to the nonorthogonality between $|\alpha\rangle$ and $|-\alpha\rangle$ [9,12]. This makes it difficult to implement quantum teleportation and gate operations in a deterministic way [12].

Toward implementations of optical quantum computation, it is important to compare existing schemes and identify the most promising and efficient ones. Ralph and Pryde made such a comparison [4] among major optical schemes including LOQC based on parity states (pLOQC) [14,15] and the cluster-state approach [16–18], CSQC, and the nonlinear Zeno protocol [19,20]. They identified pLOQC and CSQC as the best ones when considering both the loss threshold for fault-tolerant quantum computing and the resource requirements [4].

In this paper, we devise an approach based on all-optical hybrid qubits devised to combine advantages of LOQC and CSQC. In particular, we show that near-deterministic quantum teleportation can be performed using linear optics and hybrid qubits. Our approach enables one to perform near-deterministic universal gate operations for efficient scalable quantum computation. Remarkably, it outperforms LOQC and CSQC when resource requirements and error thresholds are considered together. Our work thus paves an efficient way toward the optical realization of practical quantum computation.

II. DETERMINISTIC QUANTUM TELEPORTATION AND UNIVERSAL GATE OPERATIONS USING HYBRID QUBITS

A. Hybrid optical qubits and single-qubit operations

In our approach, the orthonormal basis to define optical hybrid qubits is

$$\{|0_L\rangle = |+\rangle|\alpha\rangle, \quad |1_L\rangle = |-\rangle|-\alpha\rangle\},$$

where $|\pm\rangle = (|H\rangle \pm |V\rangle)/\sqrt{2}$ and α is assumed to be real without losing generality. As we see, this approach enables us to overcome particularly weak points of both LOQC and CSQC at the same time. The Z-basis measurement can be performed by a single measurement on either of the two physical modes. It can be done on the single-photon mode by a polarization

*h.jeong37@gmail.com

measurement on the bases $|+\rangle$ and $|-\rangle$ or on the coherent-state mode using an ancillary coherent state [9].

In our scheme, the Pauli X operation, $\hat{X}$, can be performed by applying a bit flip operation on each of the two modes. The bit flip operation on the single-photon mode, $|+\rangle \leftrightarrow |-\rangle$, is implemented by a polarization rotator, and the operation on the coherent-state mode, $|\alpha\rangle \leftrightarrow |-\alpha\rangle$, by a π phase shifter. An arbitrary Z rotation ($\hat{Z}_\theta$) is performed by applying the phase shift operation only on the single-photon mode: $\{|+\rangle,|-\rangle\} \rightarrow \{|+\rangle,e^{i\theta}|-\rangle\}$, and no operation is required on the coherent-state mode. This is a significant advantage over CSQC, in which Z rotations are highly nontrivial and cause a heavy increase of the circuit complexity [12].

B. Resource states for universal gate operations

In order to construct a universal set of gate operations, Pauli X, arbitrary Z (phase) rotation, Hadamard, and controlled-Z (CZ) gates suffice [1]. In our scheme, the necessary resource states for universal gate operations are the *hybrid pairs*, $|H\rangle|\alpha\rangle + |V\rangle|-\alpha\rangle$. We also present an alternative method using both the *two-photon pairs*, $|H\rangle|H\rangle + |V\rangle|V\rangle$, and the hybrid pairs. As we discuss, each of the two methods has its own merit, but overall the method using only hybrid pairs shows better performance. A hybrid pair can be generated in principle by performing a weak cross-Kerr nonlinear interaction between a single photon and a strong coherent state together with a displacement operation [21–23]. It has been shown that a high-fidelity cross-Kerr nonlinearity can be obtained [24–26] despite a limitation in optical fibers [27,28]. We need only small-scale hybrid pairs (e.g., $\alpha \approx 1$), of which the demonstration using gradient echo memory [25] would be experimentally feasible in the foreseeable future.

C. Near-deterministic quantum teleportation using linear optics

A teleportation protocol is required to perform Hadamard and CZ operations [29]. Using our approach, teleportation can be performed in a simple and near-deterministic manner. We emphasize that this is an extremely difficult task in the framework of LOQC because of the limited success probability of the Bell state measurement using linear optics up to 50% [6] or the required large number of modes prepared in single-photon states for a high-success teleporter [5]. It is also difficult in CSQC due to the difficulty in performing deterministic Z rotations, which is the cost of using a nonorthogonal qubit basis [12].

In our teleportation scheme, the Bell measurement for an optical hybrid qubit can be performed using two smaller Bell measurement units as shown in Fig. 1. A coherent-state Bell measurement, B_α, is implemented by a 50:50 beam splitter and two photon number parity detectors (PNPDs) [8]. It unambiguously discriminates among all four coherent Bell states, and the success probability is $1 - \exp(-2\alpha^2)$ [8]. A nondeterministic Bell measurement or type II fusion operation [6], B_{II}, identifies only two of the Bell states, e.g., $(|H\rangle|V\rangle \pm |V\rangle|H\rangle)/\sqrt{2}$, using four on-off photodetectors with success probability $1/2$ (details of B_α and B_{II} are reviewed in Appendix A).

Suppose that an unknown hybrid qubit, $|\phi\rangle = a|0_L\rangle + b|1_L\rangle$, is to be teleported using entangled channel $|\Psi_C\rangle \propto |0_L\rangle|0_L\rangle + |1_L\rangle|1_L\rangle$. The smaller Bell measurements, B_α and B_{II}, are performed in each mode together with one part of the channel $|\Psi_C\rangle$ as depicted in Fig. 1. According to the measurement results, appropriate Pauli operations are determined as shown in the table of Fig. 1, which completes the teleportation process. For example, if the "upper" detector of B_α (that employs two PNPDs) detects an odd number of photons while the "lower" one does not click, the outcome of B_α is (odd, 0) and we assign $j = 0$ and $k = 1$ as shown in the table of of Fig. 1. At the same time, in the B_{II} measurement that uses four on-off detectors, if one detector among the upper two *and* another from the lower two click, this means that the outcome is (H,H) or (H,V) or (V,H) or (V,V) in Fig. 4 of Appendix A [6]. In this case, we flip the assigned values as described in the table so that $j = 1$ and $k = 0$ are obtained. (Otherwise, j and k remain unchanged.) Finally, the feedforward operation $\hat{X}^j\hat{Z}^k$ on the output hybrid qubit in the channel completes the teleportation.

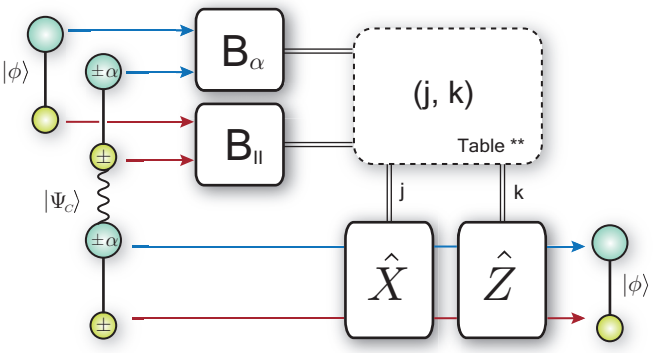

**

B_α	B_{II}	Operation
(even, 0) : j=0, k=0 (odd, 0) : j=0, k=1 (0, even) : j=1, k=0 (0, odd) : j=1, k=1	(H, H) or (V, V) or (H, V) or (V, H): Flip k ($0 \leftrightarrow 1$)	$\hat{X}^j\hat{Z}^k$
	Otherwise: No flip	
(0, 0)	(H, V) or (V, H): j=0, k=1 (H, H) or (V, V): j=1, k=1	
	Otherwise	Failure

FIG. 1. (Color online) Scheme for near-deterministic quantum teleportation for a hybrid qubit using linear optics and photon detection. An unknown hybrid qubit, $|\phi\rangle = a|0_L\rangle + b|1_L\rangle$, is teleported through channel $|\Psi_C\rangle \propto |0_L\rangle|0_L\rangle + |1_L\rangle|1_L\rangle$. B_α and B_{II} are performed on coherent-state modes and photon modes, respectively, between the qubit and one party of the channel state. All possible outcomes and corresponding feed-forward operations are presented in the table. A failure occurs when both B_α and B_{II} fail. The failure probability is found to be $P_f = \exp(-2\alpha^2)/2$. In order to perform Hadamard and CZ gates, entangled states $|Z\rangle$ and $|Z'\rangle$ should be used, respectively, instead of $|\Psi_C\rangle$.

The process will be successful unless both B_α and B_{II} fail; even though the B_α fails, the input state can be fully teleported if B_{II} is successful, as shown in the table of Fig. 1. This leads to the failure probability of

$$P_f = \tfrac{1}{2}e^{-2\alpha^2}, \tag{1}$$

which outperforms the previous schemes that require massive overheads with repetitive applications of teleporters [5,12]. For example, a 99% success rate of teleportation is achieved by encoding with $\alpha = 1.4$.

Of course, a maximally entangled state, $|\Psi_C\rangle$, in the hybrid basis is required in a quantum channel for teleportation. It can be generated, for example, by combining a hybrid pair of amplitude $\sqrt{2}\alpha$ and a two-photon pair by B_I as shown in Fig. 2(a). A state in the form of $|H\rangle|\alpha\rangle|\alpha\rangle + |V\rangle|-\alpha\rangle|-\alpha\rangle$ is obtained using a 50:50 beam splitter from the hybrid pair of amplitude $\sqrt{2}\alpha$. The B_I operation then combines it with the two-photon pair so as to generate $|\Psi_C\rangle$. Detailed analysis and an alternative generation scheme are introduced in Appendix B.

D. Hadamard and CZ operations

In order to perform the Hadamard and CZ gates, entangled states $|Z\rangle \propto |0_L\rangle|0_L\rangle + |0_L\rangle|1_L\rangle + |1_L\rangle|0_L\rangle - |1_L\rangle|1_L\rangle$ and $|Z'\rangle \propto |0000\rangle + |0011\rangle + |1100\rangle - |1111\rangle$, where $|0000\rangle = |0_L\rangle|0_L\rangle|0_L\rangle|0_L\rangle$ and so on, should be used as the teleportation channel, respectively. We present two different schemes, G_I and G_α, to generate $|Z\rangle$ as shown in Fig. 2(b). Using G_I, two B_I operations are performed on one two-photon pair and two hybrid pairs so as to link them. The other method, G_α, requires three hybrid pairs with B_I and B_α operations. One of those hybrid pairs has amplitude $\sqrt{2}\alpha$ to obtain a three-mode state $|+\rangle|\alpha\rangle|\alpha\rangle + |-\rangle|-\alpha\rangle|-\alpha\rangle$ by a 50:50 beam splitter. Appropriate feedforwards with Pauli operations are necessary for all B_I and B_α operations dependent on the measurement outcome. The four-qubit entangled state, $|Z'\rangle$, can also be generated in a similar manner with about twice the resources using either G_I or G_α. It should be noted that only hybrid pairs are required when G_α is chosen as the generation strategy, while both two photon pairs and hybrid pairs are required when using G_I. Details of all generation schemes of entangled states are presented in Appendix B. We emphasize that these states are prepared as off-line resources, while linear optical elements with photon detections are sufficient for inline operations.

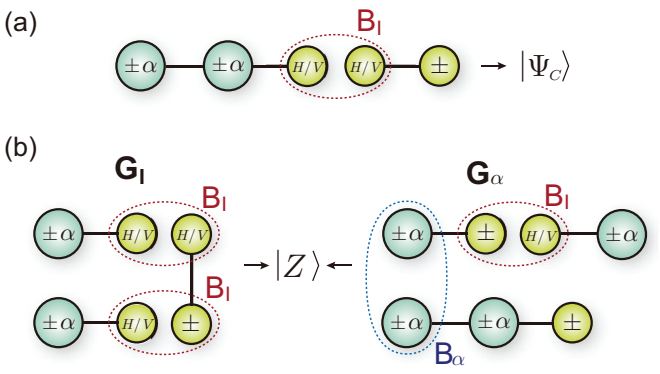

FIG. 2. (Color online) Schemes to prepare entangled channels. (a) A maximally entangled state, $|\Psi_C\rangle$, is generated using a B_I operation out of a two-photon pair and a hybrid pair of $\sqrt{2}\alpha$. In a single-photon mode, $\pm$ and $H|V$ denote bases $\{|+\rangle,|-\rangle\}$ and $\{|H\rangle,|V\rangle\}$, respectively, which can be modified by a polarization rotation before performing the B_I operation. A 50:50 beam splitter, used to split the coherent-state part with amplitude $\sqrt{2}\alpha$ into two modes, is omitted in the figure. (b) Two schemes, G_I and G_α, to generate $|Z\rangle$. In G_I, two B_I operations are performed on one two-photon pair and two hybrid pairs so as to link them. The other method, G_α, requires three hybrid pairs with B_I and B_α operations. One of those hybrid pairs has amplitude $\sqrt{2}\alpha$ to obtain a three-mode state $|+\rangle|\alpha\rangle|\alpha\rangle + |-\rangle|-\alpha\rangle|-\alpha\rangle$ by a 50:50 beam splitter (omitted in the figure). Appropriate feedforwards with Pauli operations are necessary for all B_I and B_α operations dependent on the measurement outcome.

III. PERFORMANCE ANALYSIS FOR FAULT-TOLERANT AND SCALABLE QUANTUM COMPUTATION

A. Error analysis

Errors due to photon losses are considered a major detrimental factor in optical quantum computing [4]. Some errors are immediately noticed during gate operations, which are called locatable errors [4]. Unlocatable errors are detectable only with an error-correcting code. Losses at single-photon modes are locatable by B_{II} whenever performing teleportation for Hadamard or CZ gates. Furthermore, a missing photon at a single-photon mode is immediately compensated in the output qubit $|\phi\rangle$ as far as B_α succeeds, as clearly seen in Fig. 1. However, losses at coherent-state modes may cause unlocatable errors besides locatable ones. This is due to the fact that a coherent state does not contain a definite number of photons so that it cannot be noticed when a photon is lost.

We analyze locatable and unlocatable errors with loss rate η. The analytical solution of the hybrid qubit and error rates under loss effects can be obtained using the master equation, and the full results are presented in Appendix C. Under the loss effects, the failure probability P_f for teleportation in Eq. (1) is modified to

$$P_f' = (1-\eta)\frac{e^{-2\alpha'^2}}{2} + \eta\frac{2}{1+e^{2\alpha'^2}}, \tag{2}$$

where $\alpha' = \sqrt{1-\eta}\alpha$. If a gate operation fails, the teleported qubit is assumed to experience depolarization and become fully mixed. This is equivalent to applying a random Pauli operation to the qubit; i.e., Z and X Pauli errors occur independently with equal probabilities. One can also assume that if a loss occurs in either photon or coherent-state modes, the hybrid qubit experiences a Pauli Z error with probability 1/2. We also model errors due to losses in the generation processes of $|Z\rangle$ and $|Z'\rangle$ as Pauli X and Z errors. We assume that the decrease in amplitude α by loss can be compensated whenever using the teleportation scheme by changing the amplitude of output state of the channel [12]. Based on these models and methods, we have analytically obtained probabilities of aforementioned errors in terms of η (Appendix C).

In order to realize scalable quantum computation, it should be justified that arbitrarily large computation can be implemented with small errors, which is called fault tolerance [30]. In this sense, a fault-tolerant noise threshold can be obtained such that if the amount of noise per operation is below this threshold, it is possible to realize arbitrary large-scale quantum computers with appropriate error corrections [1,31,32].

We employ an error-correction protocol with several levels of concatenation based on the circuit-based telecorrection [18]. Using the telecorrection protocol [18], noise thresholds and resource requirements in cluster-state LOQC [18], pLOQC [15], and CSQC [12] were previously investigated. In order to compare our approach with the previous ones, we follow the same analysis using the seven-qubit STEANE code [33] based on the telecorrection protocol. We assume our error model for the lowest level of concatenation. For higher levels, the noise model and error-correction protocol are identical to those of Ref. [18]. We perform a numerical simulation (Monte Carlo method using C++) for one round of the error correction for the first-level concatenation. The modified telecorrector circuit is composed of CZ, Hadamard, $|+\rangle$ creation, and X-basis measurement [12].

We carried out a series of simulations for a range of loss rate η and amplitude α. The resulting rates of unlocatable and locatable errors are used for the next level of concatenation for the error correction. If the error rates tend to zero with certain values of η and α in the limit of many levels of concatenation, fault-tolerant computing is possible with those values. In this way, the noise threshold curves are obtained.

B. Resource requirements

Once a fault-tolerant model is determined, the number of resources required for one round of error correcting may be considered as another crucial factor for scalability. We consider two-photon pairs and hybrid pairs to be resources. We estimate the number of resources required for one round of error correction in the lowest level of concatenation. It is assumed, following the estimation in Refs. [4,12], that the total number of operations in one round of the telecorrection scheme is about 1000 [4] and resources are used in each operation as the following fractions [12]: memory 0.284, Hadamard 0.098, CZ 0.343, diagonal state (hybrid-pair) 0.164, and X-basis measurement 0.111. We also assume parallel productions of resource states and no reuse of resources to avoid complicated techniques used for saving resources.

We have two types of generation schemes, G_I and G_α, which consume different numbers of resources to produce $|Z\rangle$ and $|Z'\rangle$. When generating $|Z\rangle$ by G_I, two B_I operations (the success probability of each operation is $1/2$) are used to merge one two-photon pair and two hybrid pairs (i.e., three resources). Since the success probability of the two B_I operations is $1/4$, the average number of required resources is $3 \times 4 = 12$ (i.e., four two-photon and eight hybrid pairs on average are required). In G_α, on the other hand, B_I and B_α are performed once each to merge three hybrid pairs. The success probability is then $(1 - e^{-2\alpha^2})/2$ because the failure probabilities of B_α and B_{II} is $e^{-2\alpha^2}$ and $1/2$, respectively, as discussed in Sec. II. Thus, $6/(1 - e^{-2\alpha^2})$ hybrid pairs are required in average. Likewise, when generating $|Z'\rangle$, 48 two-photon pairs and 32 hybrid pairs (80 resource states) are used in G_I, while $10/(1 - e^{-2\alpha^2})^3$ hybrid pairs are required in G_α.

Therefore, the total number of resources required for one round of error correction is obtained as $98 \times 12 + 343 \times 80 + 164 = 28\,780$ for G_I, while it is $98\lceil 6/(1 - e^{-2\alpha^2})\rceil + 343\lceil 10/(1 - e^{-2\alpha^2})^3\rceil + 164$ for G_α, which reduces to 4182 with increasing α.

C. Comparison with LOQC and CSQC

Ralph and Pryde suggest that LOQC and CSQC are the best schemes for medium-scale quantum computing considering both the fault-tolerant thresholds and the resource costs [4]. We here present the results of our numerical analysis in order to compare the performance of our scheme, when it is applied to scalable quantum computing, with LOQC and CSQC. As shown in Fig. 3(a) for G_I and G_α, the noise threshold level is obviously higher than CSQC for all region of α while it is still lower than that of pLOQC (about 2×10^{-3} [15]). The threshold peak for each generation scheme appears around $\alpha \approx 1.08$ [Fig. 3(a)]. However, further increase of α lowers the threshold level due to rapid increase of unlocatable errors, which are more difficult to correct than locatable ones using the telecorrection protocol [18]. The noise thresholds of G_I appear

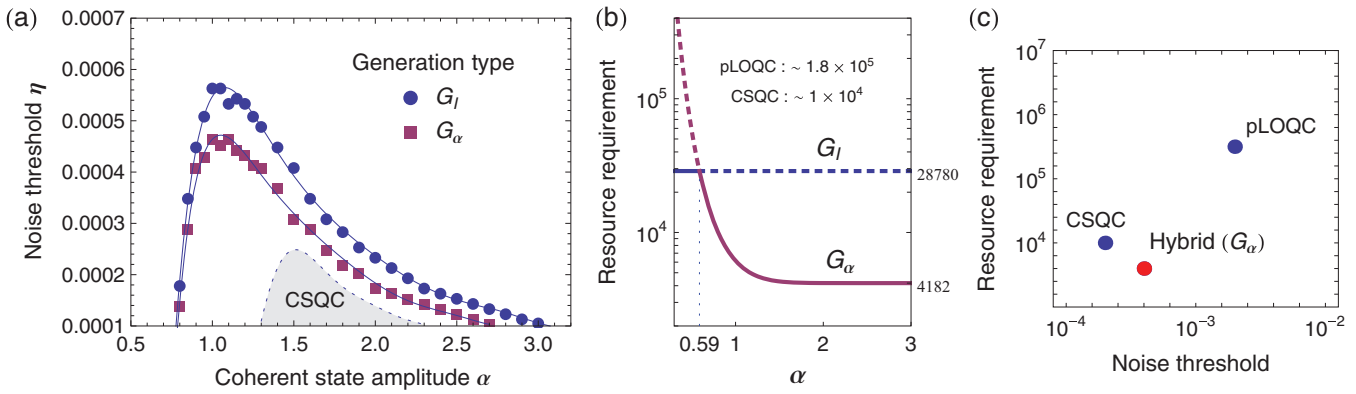

FIG. 3. (Color online) Noise thresholds and resource requirements. (a) Noise thresholds based on two generation schemes, G_I and G_α, obtained using the seven-qubit STEANE code [33]. (b) Resource requirements estimated for one round of error correction based on the telecorrection protocol. For G_I, a constant number (28 780) of resources (two-photon and hybrid pairs) are required irrespective of amplitude α, while for G_α the required number of resource states tend to decrease rapidly to 4182 with increasing α. Two curves intersect at $\alpha \approx 0.59$. We can take the lower curve between them by choosing G_α for $\alpha > 0.59$ and otherwise G_I. It shows a remarkable improvement compared to pLOQC (about 1.8×10^5 [15]) and CSQC (about 10^4 [12]). (c) Ralph-Pryde diagram [4] for the comparison with pLOQC and CSQC. The hybrid approach using G_α presented in this paper is shown to outperform pLOQC and CSQC.

to be slightly larger than those of G_α because G_α requires preparation of hybrid qubits with amplitude $\sqrt{2}\alpha$ from the beginning, as seen in Fig. 2.

Remarkably, our scheme provides a greatly reduced resource cost compared to both CSQC and pLOQC. This is partly due to the near-deterministic nature of our teleportation protocol. As presented in Fig. 3(b), resource requirements are phenomenally reduced by G_α since the success rate of B_α grows rapidly as α increases. However, the success rate of B_I is constant (1/2) and so are the resource requirements with G_I. The diagram in Fig. 3(c) clearly shows that our scheme (with G_α) shows better performance than pLOQC and LOQC when both the resource cost and the noise threshold are considered.

IV. REMARKS

In this paper, we have developed an all-optical hybrid scheme of quantum computation. We have shown that near-deterministic quantum teleportation can be performed using linear optics and hybrid qubits. Our approach enables one to perform near-deterministic universal gate operations for efficient scalable quantum computation. This approach was shown to outperform previous ones when resource requirements and error thresholds are considered together. The required *off-line* resources states are hybrid pairs in the form of $|H\rangle|\alpha\rangle + |V\rangle|-\alpha\rangle$ and only a small value of the amplitude as $\alpha \approx 1$ is required to demonstrate the maximum performance.

Toward fault-tolerant and scalable quantum computation, a crucial experimental challenge is to enhance the efficiencies of the photon detectors. In fact, efficiencies of currently available detectors [34] are far from the required levels to overcome the fault-tolerant limits. This is a critical problem in any type of optical approach to quantum computing (including LOQC and CSQC). Our scheme requires, as CSQC does, photon number-resolving detectors for parity measurements, and this is one reason that its fault-tolerant limit is still lower than pLOQC (but higher than CSQC).

Efficient preparation of the resource hybrid pairs with high fidelities along with the current progress of optical controls [4] would be the next challenge in the development of our scheme. It is known that the fidelities of hybrid pairs generated using weak nonlinearities in optical fibers are limited [27,28]. Since we only need small-scale hybrid pairs (e.g. $\alpha \approx 1$), their high-fidelity generation may be possible using gradient echo memory [25].

One may also consider the possibility that there exists more than one photon in the single-photon part of a hybrid pair (or one part of a two-photon pair) due to experimental imperfections [35]. There effects may be significantly suppressed by the B_I and B_{II} operations during the generation and inline processes. (see Appendix D for a detailed discussion).

Given the deterministic nature of our scheme and its performance over the previous ones, we expect that our work will pave an efficient way for the optical realization of scalable quantum computation. There exist experimental obstacles such as highly efficient detectors and high-fidelity resource states toward realizations of scalable quantum computation. In fact, the gaps between fault-tolerance limits and efficiencies of currently available on-off detectors and photon number-resolving detectors are still formidable [34]. On the other hand, demonstration of the teleportation scheme for a hybrid qubit would be experimentally feasible in the foreseeable future.

ACKNOWLEDGMENTS

This work was supported by a National Research Foundation of Korea (NRF) grant funded by the Korean Government (No. 2010-0018295) and the World Class University program.

APPENDIX A: REVIEW OF BELL-TYPE MEASUREMENTS

Four entangled coherent states, $|\alpha\rangle|\alpha\rangle \pm |-\alpha\rangle|-\alpha\rangle$ and $|\alpha\rangle|-\alpha\rangle \pm |-\alpha\rangle|\alpha\rangle$, can be discriminated by coherent-state Bell measurement, B_α, implemented by a 50:50 beam splitter and two photon number parity detectors (PNPDs) as shown in Fig. 4 [8,10]. The four states after passing through the Beam Splitter (BS) are

$$|\alpha\rangle|\alpha\rangle + |-\alpha\rangle|-\alpha\rangle \xrightarrow{\text{BS}} \frac{1}{\mathcal{N}_e}|\text{even}\rangle|0\rangle,$$
$$|\alpha\rangle|\alpha\rangle - |-\alpha\rangle|-\alpha\rangle \xrightarrow{\text{BS}} \frac{1}{\mathcal{N}_o}|\text{odd}\rangle|0\rangle,$$
$$|\alpha\rangle|-\alpha\rangle + |-\alpha\rangle|\alpha\rangle \xrightarrow{\text{BS}} \frac{1}{\mathcal{N}_e}|0\rangle|\text{even}\rangle,$$
$$|\alpha\rangle|-\alpha\rangle - |-\alpha\rangle|\alpha\rangle \xrightarrow{\text{BS}} \frac{1}{\mathcal{N}_o}|0\rangle|\text{odd}\rangle,$$

where $|\text{even}\rangle = \mathcal{N}_e(|\sqrt{2}\alpha\rangle + |-\sqrt{2}\alpha\rangle)$ and $|\text{odd}\rangle = \mathcal{N}_o(|\sqrt{2}\alpha\rangle - |-\sqrt{2}\alpha\rangle)$ (with normalization factors $\mathcal{N}_e$ and $\mathcal{N}_o$) contain only even and odd photon number states, respectively. Therefore, parity measurements on each output mode enable one to discriminate between the four Bell states.

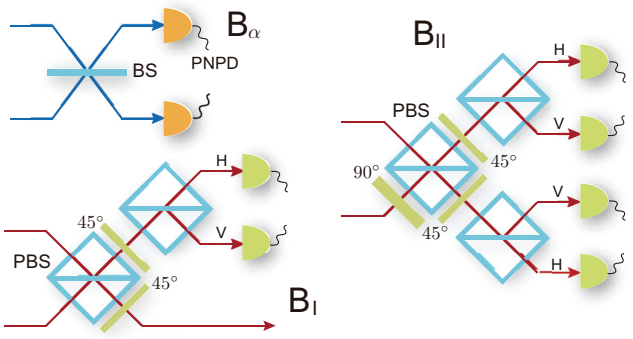

FIG. 4. (Color online) Three Bell-type measurement elements used for our scheme. A coherent-state Bell measurement, B_α, is implemented by a 50:50 BS and two photon number parity detectors (PNPD) [8]. B_α unambiguously discriminates between all four Bell states and the success probability is $1 - \exp(-2|\alpha|^2)$. It fails only when no photon is detected at both the detectors. A type I fusion operation [17], B_I, is implemented by polarizing beam splitters (PBSs), wave plates, and photon detectors. It effectively performs $|+\rangle\langle H|\langle H| \pm |-\rangle\langle V|\langle V|$ with a success probability 1/2 when only one photon is detected at either detector [17]. A nondeterministic Bell measurement or modified version of the typeII fusion operation, B_{II}, identifies only two of the Bell states, $|H\rangle|V\rangle \pm |V\rangle|H\rangle$, with success probability 1/2. It succeeds only when one detector from the upper two and another from the lower two click at the same time.

A failure occurs when no photon is detected in both the detectors due to the nonzero overlap of $\langle 0| \pm \sqrt{2}\alpha\rangle = e^{-\alpha^2}$.

When B_α is performed on two hybrid qubits, $|\psi\rangle = a|+\rangle|\alpha\rangle + b|-\rangle|-\alpha\rangle$ and $|\psi'\rangle = a'|+\rangle|\alpha\rangle + b'|-\rangle|-\alpha\rangle$, coherent-state modes of two qubits are mixed by the 50:50 BS, such that the state evolves as

$$\begin{aligned}|\psi\rangle|\psi'\rangle \xrightarrow{\text{BS}} & \frac{1}{2\mathcal{N}_e}(aa'|+\rangle|+\rangle + bb'|-\rangle|-\rangle)|\text{even}\rangle|0\rangle \\ & + \frac{1}{2\mathcal{N}_o}(aa'|+\rangle|+\rangle - bb'|-\rangle|-\rangle)|\text{odd}\rangle|0\rangle \\ & + \frac{1}{2\mathcal{N}_e}(ab'|+\rangle|-\rangle + ba'|-\rangle|+\rangle)|0\rangle|\text{even}\rangle \\ & - \frac{1}{2\mathcal{N}_o}(ab'|+\rangle|-\rangle - ba'|-\rangle|+\rangle)|0\rangle|\text{odd}\rangle,\end{aligned}$$

and the four possible states of remaining photon modes can be discriminated from the results of the parity measurements on the output modes of the BS. We note that its failure probability

$$|\langle 0|\langle 0|\psi\rangle|\psi'\rangle|^2 = e^{-2\alpha^2}(|a|^2 + |b|^2)(|a'|^2 + |b'|^2) = e^{-2\alpha^2}$$

is lower than that obtained in CSQC [8–12] due to the orthonormality of the hybrid qubit basis, i.e., $|a|^2 + |b|^2 = 1$.

In the single-photon mode, two types of Bell measurements are used in Fig. 4. A type I fusion operation B_I [17] performs a partial Bell measurement on the polarization states of photons. Its measurement outcome is either H (when a photon is detected at the upper detector) or V (when a photon is detected at the lower detector), which determines the operation actually carried out as $|+\rangle\langle H|\langle H| - |-\rangle\langle V|\langle V|$ and $|+\rangle\langle H|\langle H| + |-\rangle\langle V|\langle V|$ for H and V clicks, respectively. It fails when two photons or no photon is detected at detectors, which occurs with probability 1/2.

A type II fusion operation B_{II} [17] performs an incomplete Bell measurement with which only two out of the four Bell states are distinguished [36,37]. It can be implemented by a polarizing beam splitter (PBS), wave plates, and photon detectors. It succeeds with probability 1/2 when one detector from the upper two and another from the lower two click at the same time in Fig. 4 so that two Bell states can be identified from the results: $|H\rangle|V\rangle - |V\rangle|H\rangle$ for the clicks (H,H) or (V,V), and $|H\rangle|V\rangle + |V\rangle|H\rangle$ for (H,V) or (V,H).

APPENDIX B: GENERATING ENTANGLED STATES

A maximally entangled state of hybrid qubits $|\Psi_C\rangle \propto |0_L\rangle|0_L\rangle + |1_L\rangle|1_L\rangle$ can be generated by either of the two schemes, G_I or G_α, described in Fig. 3. In G_I, a hybrid pair with $\sqrt{2}$ times larger amplitude $|\psi_{\sqrt{2}\alpha}\rangle = |H\rangle|\sqrt{2}\alpha\rangle + |V\rangle|-\sqrt{2}\alpha\rangle$ and a two-photon pair $|H\rangle|+\rangle + |V\rangle|-\rangle$ are merged by the B_I operation:

$$(|\alpha\rangle|\alpha\rangle|H\rangle + |-\alpha\rangle|-\alpha\rangle \underbrace{|V\rangle)(|H\rangle}_{B_I}|+\rangle + |V\rangle|-\rangle),$$

where the coherent-state mode was split into two modes by a 50:50 BS. Then, the resulting state is associated with the measurement outcome of B_I as

$$\begin{aligned}&\text{(H) Click}: |+\rangle|\alpha\rangle|+\rangle|\alpha\rangle - |-\rangle|-\alpha\rangle|-\rangle|-\alpha\rangle, \\ &\text{(V) Click}: |+\rangle|\alpha\rangle|+\rangle|\alpha\rangle + |-\rangle|-\alpha\rangle|-\rangle|-\alpha\rangle,\end{aligned}$$

TABLE I. Feedforwards dependent on the results of B_α

Measurement outcomes of B_α	Pauli operations
(even, 0)	$\mathbb{1}$
(odd, 0)	$\hat{Z}$
(0, even)	$\hat{X}$
(0, odd)	$\hat{Z}$ and $\hat{X}$
(0, 0)	Failure

and thus, by applying a Pauli Z operation on any qubit mode when the outcome is (H), we obtain $|\Psi_C\rangle$ whenever B_I operation succeeds with probability 1/2.

In G_α, two $|+\rangle|\alpha\rangle|\alpha\rangle + |-\rangle|-\alpha\rangle|-\alpha\rangle$ states, obtained by applying a 50:50 BS to a hybrid pair with amplitude $\sqrt{2}\alpha$, are merged by the B_α operation. An appropriate Pauli operations dependent on the measurement outcome are applied on the remaining part so that the same state $|\Psi_C\rangle$ is produced whenever B_α succeeds with probability $1 - e^{-2\alpha^2}$ (see Table I). For example, when the measured outcome is (odd, 0), the resulting state is $|+\rangle|\alpha\rangle|+\rangle|\alpha\rangle - |-\rangle|-\alpha\rangle|-\rangle|-\alpha\rangle$ and a Pauli Z operation on one qubit changes it to $|\Psi_C\rangle$.

A hybrid entangled state $|Z\rangle \propto |0_L\rangle|0_L\rangle + |0_L\rangle|1_L\rangle + |1_L\rangle|0_L\rangle - |1_L\rangle|1_L\rangle$ can be generated by either G_I or G_α as shown in Fig. 5. In G_I, one two-photon pair in $|H\rangle|+\rangle + |V\rangle|-\rangle$ and two hybrid pairs in $|H\rangle|\alpha\rangle + |V\rangle|-\alpha\rangle$ are merged by two B_I operations, and a Pauli Z operation is applied on the outgoing mode of each B_I when the measurement outcome is (H). Then, $|Z\rangle$ is obtained when both B_I operations succeed with probability 1/4. In G_α, three hybrid pairs are merged by B_I and B_α as shown in Fig. 5. Here again a Pauli Z operation is applied on the outgoing mode when the outcome of B_I is (H), and likewise appropriate Pauli operations (see Table I) are also applied after B_α operation on the remaining qubit (denoted by dotted circle in Fig. 5). Thus the total success probability is given as $(1 - e^{-2\alpha^2})/2$ since B_I and B_α are used once each in the generation process.

A four-qubit entangled state $|Z'\rangle \propto |0_L\rangle|0_L\rangle|0_L\rangle|0_L\rangle + |0_L\rangle|0_L\rangle|1_L\rangle|1_L\rangle + |1_L\rangle|1_L\rangle|0_L\rangle|0_L\rangle - |1_L\rangle|1_L\rangle|1_L\rangle|1_L\rangle$ can also be generated by either G_I or G_α as shown in Fig. 5. Two photon pairs and one $|Z\rangle$ state (with $\sqrt{2}$ times larger α) are merged by two B_I operations in G_I, while two hybrid pairs and one $|Z\rangle$ state (all have $\sqrt{2}$ times larger α) are merged by two B_α operations in G_α. All B_I and B_α are followed by appropriate Pauli operations dependent on their outcomes. The success probability of G_I is $(1/2)^4$ as it uses four B_I operations, while it is $(1 - e^{-2\alpha^2})^3/2$ for G_α as it uses one B_I and three B_α operations.

APPENDIX C: ERROR PROBABILITIES IN LOSSY ENVIRONMENT

In our numerical analysis, we consider errors caused by photon losses, which are major obstacles to practical optical quantum computation. The evolution of optical qubits in a lossy environment can be described by solving a master equation $d\rho/dt = \gamma(\hat{J} + \hat{L})\rho$ with $\hat{J}\rho = \sum_i \hat{a}_i \rho \hat{a}_i^\dagger$ and $\hat{L}\rho = -\frac{1}{2}\sum_i(\hat{a}_i^\dagger \hat{a}_i \rho + \rho \hat{a}_i^\dagger \hat{a}_i)$ [38], where $\hat{a}_i(\hat{a}_i^\dagger)$ is the annihilation (creation) operator for ith mode. If the initial state is a hybrid

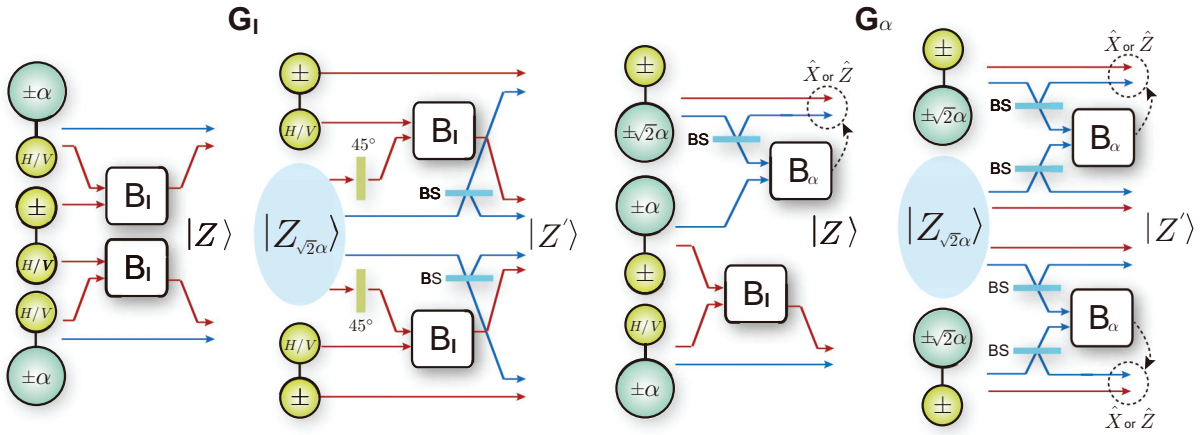

FIG. 5. (Color online) Two schemes, G_I and G_α, for generating $|Z\rangle$ and $|Z'\rangle$ states. In a single-photon mode, $\pm$ and $H|V$ denote bases $\{|+\rangle,|-\rangle\}$ and $\{|H\rangle,|V\rangle\}$, respectively, which can be modified by a polarization rotation. A Pauli Z operation (omitted in figure) is performed on the output qubit of B_I when the measurement outcome of B_I is (H). Likewise, for B_α appropriate Pauli operations are performed on the remaining qubit (denoted by dotted circle) according to the measurement results as shown in Table I.

qubit $|\psi\rangle = a|+\rangle|\alpha\rangle + b|-\rangle|-\alpha\rangle$, it evolves into a mixed state,

$$|\psi\rangle \xrightarrow{\eta} (1-\eta)\left(\frac{1+e^{-2\eta\alpha^2}}{2}|\psi'^{+}\rangle\langle\psi'^{+}| + \frac{1-e^{-2\eta\alpha^2}}{2}|\psi'^{-}\rangle\langle\psi'^{-}|\right) + \eta\left(\frac{1}{2\mathcal{N}_{a,b}^{+2}}|\phi^{+}\rangle\langle\phi^{+}| + \frac{1}{2\mathcal{N}_{a,b}^{-2}}|\phi^{-}\rangle\langle\phi^{-}|\right), \quad \text{(C1)}$$

where the loss rate is defined as $\eta = 1 - e^{-\gamma t}$. Here $|\psi'^{\pm}\rangle = a|+\rangle|\alpha'\rangle \pm b|-\rangle|-\alpha'\rangle$ with $\alpha' = \sqrt{1-\eta}\alpha$ are possible resulting states of a hybrid qubit when only the amplitude of the coherent state is reduced, while $|\phi^{\pm}\rangle = \mathcal{N}_{a,b}^{\pm}|0\rangle(a|\alpha'\rangle + b|-\alpha'\rangle)$ with normalization factors $\mathcal{N}_{a,b}^{\pm}$ are possible remaining coherent states when loss occurs in the single-photon mode. The loss rate η is considered a known value and the states $|\psi'^{+}\rangle$ and $|\phi^{+}\rangle$ do not contain any logical errors. On the other hand, $|\psi'^{-}\rangle$ and $|\phi^{-}\rangle$ contain Pauli Z errors. Note that the probabilities of the states $|\phi^{\pm}\rangle$ depend on a and b since coherent state qubits are carrying information in a nonorthogonal basis. We here choose the worst case of the error rate, which is obtained from the condition of the minimum value of $\mathcal{N}_{a,b}^{-}$. This results in $\mathcal{N}_{a,b}^{\pm} = 1$ and the state (C1) becomes

$$\left((1-\eta)\frac{1+e^{-2\eta\alpha^2}}{2}|\psi'^{+}\rangle\langle\psi'^{+}| + \frac{\eta}{2}|\phi^{+}\rangle\langle\phi^{+}|\right) + \left((1-\eta)\frac{1-e^{-2\eta\alpha^2}}{2}|\psi'^{-}\rangle\langle\psi'^{-}| + \frac{\eta}{2}|\phi^{-}\rangle\langle\phi^{-}|\right)_Z, \quad \text{(C2)}$$

where the last two terms represent the states conveying Pauli Z errors.

Based on the above result, we can investigate all possible errors caused by losses in our scheme. The failure probability of teleportation, P_f in Eq. (1), is changed to P_f' in Eq. (2) by losses. The modified error probability P_f' is a weighted sum of the error probabilities obtained using the loss rate η for the photon in the single-photon mode and the reduced amplitude of the coherent state α'. The component in the second term, $2/(1+e^{2\alpha'^2})$, corresponds to the failure probability of the coherent-state teleportation in the presence of loss obtained in Ref. [12].

If a Hadamard or CZ gate fails, this means that a hybrid-Bell measurement failed (or both the hybrid-Bell measurements failed in the case of a CZ gate). In this case, it can be shown that the output qubit(s) experience depolarization and become fully mixed. This can be modeled in our scheme by applying a random Pauli operation to the qubit, i.e.; Z and X Pauli errors occur independently with equal probabilities.

The loss in a photon part can be detected whenever performing a B_{II} operation in teleportation and the loss is compensated once the teleportation succeeds (i.e., if either B_{II} or B_α is successful done in the hybrid-Bell measurement). If photon loss at a photon part (which occurs with probability η) is noticed, it means that a Pauli Z error might have occurred with probability $1/2$ as implied in Eq. (2).

We also consider errors that may occur in quantum memory that is used to store qubits that are not undergoing gate operations. In quantum memory, losses in either photon or coherent-state mode induce Pauli Z errors with the rate

$$p = (1-\eta)\frac{1-e^{-2\eta\alpha^2}}{2} + \frac{\eta}{2} = \frac{1}{2}\{1-(1-\eta)e^{-2\eta\alpha^2}\},$$

which is obtained by summing the probabilities of the last two terms in Eq. (C2).

The entangled states $|Z\rangle$ and $|Z'\rangle$ are necessary resources for Hadamard and CZ gates in our scheme. Losses in the generation processes of $|Z\rangle$ and $|Z'\rangle$ may cause errors in output qubits of Hadamard and CZ gates. We consider these errors by assuming that losses occur immediately after the resource states are produced [12,18]. In this model, photon loss at one qubit in $|Z\rangle$ induces a Pauli Z error, while loss at the other qubit induces a Pauli X error in a teleportation process for a Hadamard gate. The error probability for both Pauli Z and X errors is p, which obtained exactly in the same way as the one obtained in quantum memory from Eq. (2). Losses in any qubit

of $|Z'\rangle$ induce a Pauli Z error in a CZ gate with probability p per qubit.

The preparation of the diagonal qubits (i.e., hybrid pairs) is required for the telecorrection protocol. We also consider possible errors in the preparation of a diagonal qubit by assuming that loss occurs immediately after its generation so that it may convey a Pauli Z error with probability p. It is also assumed that there is no additional error caused by the X-basis measurement used in the telecorrection protocol.

APPENDIX D: EFFECTS OF MULTIPHOTON CONTRIBUTIONS

Due to experimental imperfections, there could be more than one photon in one part of a two-photon pair (or in the single-photon part of a hybrid pair). First, in the off-line preparation process using B_I, multiphotons in the single-photon part can be partially detected (for example, by the case when detectors simultaneously click in a B_I operation), and such cases can simply be discarded. Such errors only result in a slight increase of the resource requirement (given that the multiportion contribution is slight compared to the single-photon contribution, which is a reasonable assumption [35,39]).

First, we point out that roughly half of the multiphoton contributions will be discarded by B_I during the generation process. To explain this, we use an approximate approach: let us assume that the generated state (for the case of a two-photon pair but the same analysis apply a hybrid pair) is

$$\propto|H\rangle|H\rangle + |V\rangle|V\rangle + \lambda(|2H\rangle|2H\rangle + |2V\rangle|2V\rangle),$$

where $|2H\rangle$ ($|2V\rangle$) is a two-photon state with the horizontal (vertical) polarization and λ is assumed to be a small value. Considering a typical down-conversion process, we can assume that λ is very small and the probability of having three photons (or more) in one mode is negligible [35,39]. We also ignore λ^2 factors in the following calculations because λ is already very small. Due to the symmetry, it is sufficient to consider the following four possible possibilities (out of total eight), $|2H\rangle|V\rangle$ or $|2V\rangle|V\rangle$ or $|2H\rangle|H\rangle$ or $|2V\rangle|V\rangle$ (upper and lower modes in order), as the input to the PBS of the B_I process shown in Fig. 4.

The two PBSs used for a B_I process are assumed to pass "H" polarizations and to reflect "V". Note also that detectors used for a standard B_I process require single-photon detectors that discriminate among 0, 1, and more than 1 photon [17]. For the first two cases, $|2H\rangle|V\rangle$ or $|2V\rangle|V\rangle$, all the photons go to either the upper direction together or the lower by the first PBS in Fig. 4. These cases are all failures and are not much different from those without multiphoton contributions. For the third case, $|2H\rangle|H\rangle$, one photon goes to the upper part and the two photons go to the lower part. This result is considered a "success" and the two-photon contribution goes into the inline process. For the fourth case, $|2V\rangle|V\rangle$, the two photons go to the upper part and one photon goes to the lower part. The two detectors then recognize that there exists more than one photon. (Note that even though the detectors used for the B_I operation discriminate between a single photon and two or more photons, they cannot resolve more than two photons.) This case is a failure and is simply discarded. Therefore, we can conclude that the multiphoton contributions are reduced to about half by the B_I operations during the resource-generation stage (with a slight increase of the resource cost).

Next, for the remaining multiphoton contributions in the inline process, we can make the same analysis as above with the four cases for the two input modes. It should be noted that a standard B_{II} operation use four *on-off* detectors, and two of those detectors click when the result is a success. If the "surplus" photon goes to one of those two detectors, the result is considered as a success, but success events possibly convey unlocatable Pauli Z error with a probability $1/2$. On the other hand, if the "surplus" photon goes to one of the other two detectors, the result is a failure, i.e., a locatable error. For example, if the input state is $|2H\rangle|V\rangle + |2V\rangle|H\rangle$, all possible cases for the success events in front of the second PBSs are $|H\rangle|2H\rangle$, $|2H\rangle|H\rangle$, $|V\rangle|2V\rangle$, $|2V\rangle|V\rangle$, $|H\rangle|2V\rangle$, $|2H\rangle|V\rangle$, $|V\rangle|2H\rangle$, and $|2V\rangle|H\rangle$. If (H,V) or (V,H) clicks occur at the detectors, with probability $1/2$, the result is a "correct" success and the multiphoton contribution will simply disappear at the detectors. However, if (H,H) or (V,V) events occurs, the result is an "incorrect" success and it will deliver an unnoticed Pauli Z error to the teleported qubit. All other cases in front of the second PBSs such as $|H\rangle|HV\rangle$, $|HV\rangle|H\rangle$, $|V\rangle|HV\rangle$, and $|HV\rangle|V\rangle$ are detected as failures.

Finally, when there is photon loss, there is some additional possibility of errors caused by the multiphoton contributions. For example, the multiphoton contribution may cause a "click at a wrong detector" and a "photon missing at a correct detector." This type of error cannot be noticed and thus is an unlocatable error.

In summary, the multiphoton contributions play a role to increase the resource cost and decrease the noise threshold. However, based on the discussions above, we can expect that the effects of multiphoton contributions are relatively very small because most of them would have been discarded by B_I or detected by B_{II} (and some even disappear by B_{II} without any cost) during the generation and inline processes. We also point out that, of course, such multiphoton effects, which are not considered in most of the references, are present not only in our scheme but also in any LOQC-type approaches (including pLOQC) where two-photon pairs, generated by the parametric down-conversion, are used as resources [40].

[1] M. A. Nielsen and I. L. Chuang, *Quantum Computation and Quantum Information* (Cambridge University Press, Cambridge, 2000).
[2] J. L. O'Brien, Science **318**, 1567 (2007).
[3] P. Kok, W. J. Munro, K. Nemoto, T. C. Ralph, J. P. Dowling, and G. J. Milburn, Rev. Mod. Phys. **79**, 135 (2007).
[4] T. C. Ralph and G. J. Pryde, Prog. Opt. **54**, 209 (2010).
[5] E. Knill, R. Laflamme, and G. J. Milburn, Nature (London) **409**, 46 (2001).
[6] J. Calsamiglia and N. Lütkenhaus, App. Phys. B **72**, 67 (2001).
[7] W. P. Grice, Phys. Rev. A **84**, 042331 (2011).

[8] H. Jeong, M. S. Kim, and J. Lee, Phys. Rev. A **64**, 052308 (2001).
[9] H. Jeong and M. S. Kim, Phys. Rev. A **65**, 042305 (2002).
[10] H. Jeong and M. S. Kim, Quantum Inf. Comp. **2**, 208 (2002).
[11] T. C. Ralph, A. Gilchrist, G. J. Milburn, W. J. Munro, and S. Glancy, Phys. Rev. A **68**, 042319 (2003).
[12] A. P. Lund, T. C. Ralph, and H. L. Haselgrove, Phys. Rev. Lett. **100**, 030503 (2008).
[13] A. Ourjoumtsev, H. Jeong, R. Tualle-Brouri, and P. Grangier, Nature (London) **448**, 784 (2007).
[14] T. C. Ralph, A. J. F. Hayes, and A. Gilchrist, Phys. Rev. Lett. **95**, 100501 (2005).
[15] A. J. F. Hayes, H. L. Haselgrove, A. Gilchrist, and T. C. Ralph, Phys. Rev. A **82**, 022323 (2010).
[16] M. A. Nielsen, Phys. Rev. Lett. **93**, 040503 (2004).
[17] D. E. Browne and T. Rudolph, Phys. Rev. Lett. **95**, 010501 (2005).
[18] C. M. Dawson, H. L. Haselgrove, and M. A. Nielsen, Phys. Rev. A **73**, 052306 (2006).
[19] J. D. Franson, B. C. Jacobs, and T. B. Pittman, Phys. Rev. A **70**, 062302 (2004).
[20] P. M. Leung and T. C. Ralph, New J. Phys. **9**, 224 (2007).
[21] K. Nemoto and W. J. Munro, Phys. Rev. Lett. **93**, 250502 (2004).
[22] H. Jeong, Phys. Rev. A **72**, 034305 (2005).
[23] W. J. Munro, K. Nemoto, and T. P. Spiller, New J. Phys. **7**, 137 (2005).
[24] B. He, Q. Lin, and C. Simon, Phys. Rev. A **83**, 053826 (2011).
[25] M. Hosseini, S. Rebić, B. M. Sparkes, J. Twamley, B. C. Buchler, and P. K. Lam, arXiv:1112.2010.
[26] C. Chudzick, I. L. Chuang, and J. H. Shapiro, arXiv:1202.6640.
[27] J. H. Shapiro, Phys. Rev. A **73**, 062305 (2006).
[28] J. H. Shapiro and M. Razavi, New J. Phys. **9**, 16 (2007).
[29] D. Gottesman and I. L. Chuang, Nature (London) **402**, 390 (1999).
[30] P. W. Shor, in *Proceedings of the 37th Annual Symposium on Fundamentals of Computer Science* (IEEE Computer Society Press, Los Alamotios, CA, 1996), pp. 56–65.
[31] A. M. Steane, Phys. Rev. A **68**, 042322 (2003).
[32] E. Knill, Nature (London) **434**, 39 (2005).
[33] A. M. Steane, Phys. Rev. A **54**, 4741 (1996).
[34] M. D. Eisaman, J. Fan, A. Migdall, and S. V. Polyakov, Rev. Sci. Instrum. **82**, 071101 (2011).
[35] P. G. Kwiat, K. Mattle, H. Weinfurter, A. Zeilinger, A. V. Sergienko, and Y. Shih, Phys. Rev. Lett. **75**, 4337 (1995).
[36] H. Weinfurt, Europhys. Lett. **8**, 559 (1994).
[37] N. Lütkenhaus, J. Calsamiglia, and K.-A. Suominen, Phys. Rev. A **59**, 3295 (1999).
[38] S. J. D. Phoenix, Phys. Rev. A **41**, 5132 (1990).
[39] A. Ourjoumtsev, R. Tualle-Brouri, and Ph Grangier, Phys. Rev. Lett. **96**, 213601 (2006).
[40] P. Kok and B. W. Lovett, *Introduction to Optical Quantum Information Processing* (Cambridge University Press, Cambridge, 2010).